Synthetic, Structural, Chemical, and Electrochemical Studies of the Metallatricarbadecaboranyl Analogues of Ferrocene, Ruthenocene, and Osmocene and the Observation of a Reversible $\eta^6-\eta^4$ Tricarbadecaboranyl Coordination that Is Analogous to the $\eta^5-\eta^3$ Cyclopentadienyl Ring-Slippage Process

Bhaskar M. Ramachandran,[1] Sabrina M. Trupia,[2] William E. Geiger,*[,2] Patrick J. Carroll,[1] and Larry G. Sneddon*[,1]

Departments of Chemistry, University of Pennsylvania, Philadelphia, Pennsylvania 19104-6323, and University of Vermont, Burlington, Vermont 05405

Received September 12, 2002

The tricarbadecaboranyl anions, 6-R-*nido*-5,6,9-$C_3B_7H_9^-$ (R = CH_3 or C_6H_5), have been employed to produce a series of metallatricarbadecaboranyl analogues of the group VIII metallocenes, $(\eta^5\text{-}C_5H_5)_2M$, M = Fe, Ru, and Os, including 1-(η^5-C_5Me_5)-2-Me-*closo*-1,2,3,4-$RuC_3B_7H_9$ (**3**), *commo-Ru*-(2-Me-*closo*-1,2,3,4-$RuC_3B_7H_9)_2$ (**4**), *commo-Os*-(4′-Me-*closo*-1′,2′,3′,4′-$OsC_3B_7H_9$)(2-Me-*closo*-1,2,3,4-$OsC_3B_7H_9$) (**5**), *commo-Os*-(2-Me-*closo*-1,2,3,4-$OsC_3B_7H_9)_2$ (**6**), 1-(η^5-C_5H_5)-2-Ph-*closo*-1,2,3,4-$FeC_3B_7H_9$ (**7**), and 1-(η^5-C_5Me_5)-2-Ph-*closo*-1,2,3,4-$RuC_3B_7H_9$ (**8**). In the mixed ligand complexes **3**, **7**, and **8**, formal Fe^{2+} and Ru^{2+} ions are sandwiched between the tricarbadecaboranyl and cyclopentadienyl monoanionic ligands, while in complexes **4**, **5**, and **6** the Ru^{2+} and Os^{2+} ions are sandwiched between two tricarbadecaboranyl ligands. In all complexes, the metals are η^6-coordinated to the puckered six-membered face of the tricarbadecaboranyl cage. Reaction of **7** with $Cr(CO)_6$ resulted in the formation of the arene-substituted complex 1-(η^5-C_5H_5)-2-[(η^6-C_6H_5)$Cr(CO)_3$]-*closo*-1,2,3,4-$FeC_3B_7H_9$ (**9**). Complexes **3** and **7** were also found to undergo reversible cage-slippages between the $\eta^6-\eta^4$ coordination modes during the association−dissociation reactions of these complexes with *tert*-butylisocyanide to produce 8-(η^5-C_5Me_5)-8-($CNBu^t$)-9-Me-*nido*-8,7,9,10-$RuC_3B_7H_9$ (**10**) and 8-(η^5-C_5H_5)-8-($CNBu^t$)-9-Ph-*nido*-8,7,9,10-$FeC_3B_7H_9$ (**11**), respectively. This reversible $\eta^6-\eta^4$ coordination is analogous to the $\eta^5-\eta^3$ ring-slippage process that is proposed to occur in related reactions of cyclopentadienyl-metal complexes. Electrochemical studies revealed that the tricarbadecaboranyl compounds undergo reversible one-electron oxidations and two successive one-electron reductions. Comparison of oxidation $E_{1/2}$ values for Cp and $RC_3B_7H_9$ analogues indicates a comparative electronic effect of +0.44 V for the tricarbadecaboranyl group. Reduction $E_{1/2}$ values indicate a stabilization energy of 1.2−1.7 V in excess of the comparative electronic effect. It is likely that the overall ligand-induced stabilization of low metal oxidation states arises in part from redox-induced hapticity changes of the tricarbadecaboranyl ligand. Formal M^0 dianions are detected that have no precedence in the metallocenes.

Introduction

We have previously demonstrated[3] that, because of their equivalent charges and formal electron-donating abilities, the coordination properties of the tricarbadecaboranyl, 6-Me-*nido*-5,6,9-$C_3B_7H_9^-$,[4] and the cyclopentadienide monoanions (Figure 1) are in many ways similar, but that metallatricarbadecaboranyl complexes have significantly greater oxidative, chemical, thermal, and hydrolytic stabilities than their metallocene counterparts. For example, we recently reported[3g] the formation of a series of vanadatricarbadecaboranyl analogues, i.e., $(Me\text{-}C_3B_7H_9)_2V$, of vanadocene $(\eta^5\text{-}C_5H_5)_2V$, that are, unlike vanadocene, both air- and water-stable. In this paper we report the synthetic, structural, chemical, and

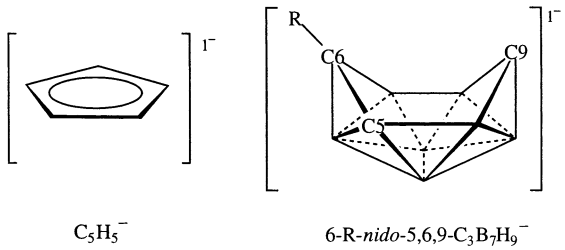

$C_5H_5^-$ 6-R-*nido*-5,6,9-$C_3B_7H_9^-$

Figure 1. Comparison of the structures of the cyclopentadienyl and tricarbadecaboranyl anions.

(1) University of Pennsylvania.
(2) University of Vermont.

10.1021/om020757u CCC: $22.00
Publication on Web 10/15/2002

electrochemical studies of a series of new ferra-, ruthena-, and osmatricarbadecaboranyl analogues of ferrocene, ruthenocene, and osmocene that again illustrate the unique properties of the tricarbadecaboranyl ligand. In addition, we also report the discovery of a reversible cage-slippage of the tricarbadecaboranyl ligand between $\eta^6-\eta^4$ coordination modes that occurs during the association−dissociation reactions of several of these complexes with *tert*-butylisocyanide.[5] This process is analogous to the $\eta^5-\eta^3$ ring-slippage that is proposed to occur in related reactions of cyclopentadienyl-metal complexes.[6]

Experimental Section

General Synthetic Procedures and Materials. Unless otherwise noted, all reactions and manipulations were performed in dry glassware under a nitrogen or argon atmosphere using the high-vacuum or inert-atmosphere techniques described by Shriver.[7] Li^+(6-Me-*nido*-5,6,9-$C_3B_7H_9^-$) (**1**$^-$)[3a,g,4] and Li^+(6-Ph-*nido*-5,6,9-$C_3B_7H_9^-$) (**2**$^-$)[8] were prepared by the reported methods. LiH, $[Ru(1,5\text{-}C_8H_{12})Cl_2]_x$, ($\eta^5$-$C_5H_5$)Fe(CO)$_2$I, $Na_2(OsCl_6)\cdot 4H_2O$, $Cr(CO)_6$, dibutyl ether, *tert*-butylisocyanide, benzonitrile, and $(Cp^*RuCl_2)_x$ polymer were purchased from Strem or Aldrich and used as received. Spectrochemical grade glyme, diethyl ether, tetrahydrofuran, toluene, acetonitrile, dichloromethane, and hexanes were purchased from Fisher or EM Science. Glyme and tetrahydrofuran were freshly distilled from sodium-benzophenone ketyl prior to use. Acetonitrile was dried over P_2O_5, transferred onto activated 4 Å molecular sieves, and stored under vacuum. All other solvents were used as received unless noted otherwise.

Preparative thin-layer chromatography was conducted on 0.5 mm (20 × 20) silica gel F-254 plates (Merck-5744). The yields of all metallatricarbaborane products are calculated on the basis of the starting metal reagents.

Physical Methods. The ^{11}B NMR at 64.2 MHz and ^{1}H NMR at 200 MHz were obtained on a Bruker AC 200 Fourier transform spectrometer equipped with appropriate decoupling accessories. ^{11}B NMR at 160.5 MHz, ^{13}C NMR at 125.7 MHz, and ^{1}H NMR at 500 MHz were obtained on a Bruker AM-500 spectrometer equipped with the appropriate decoupling accessories. All ^{11}B chemical shifts are referenced to $BF_3\cdot OEt_2$ (0.0 ppm), with a negative sign indicating an upfield shift. All proton chemical shifts were measured relative to internal residual protons from lock solvents (99.5% C_6D_6 and 99.9% CD_2Cl_2), then referenced to $(CH_3)_4Si$ (0.0 ppm). NMR data are summarized in Table 1.

Table 1. NMR Data

compound	nucleus	δ (mult, J (Hz), assignt)
12[3a]	$^{11}B^{a,b}$	2.6 (d, 158), 1.9 (d, 172), −7.4 (d, 147),−10.6 (d, 147), −24.6 (d, 145), −27.7 (d, 156),−32.2 (d, 157)
	$^1H^{a,c}$	6.60 (br s, C3H), 3.85 (s, Cp), 2.57 (s, Me), 0.71 (s br, C4H)
3	$^{11}B^{a,b}$	3.5 (d, 185), 2.3 (d, 165), −6.4 (d, 148), −7.8 (d, 148), −27.4 (d, 126), −28.2 (2, d, 154)
	$^1H^{a,c}$	4.78 (br s, C3H), 2.28 (s, Me), 1.35 (s, Cp*), 1.27 (br s, C4H)
4	$^{11}B^{a,b}$	9.2 (d, 163), 4.1 (d, 170), 1.9 (d, 154), −4.8 (d, 162), −22.6 (d, 184), −23.8 (d, 169), −27.0 (d, 159)
	$^1H^{a,c}$	6.05 (s, C3H), 2.14 (s, Me), 1.73 (s, C4H)
5	$^{11}B^{a,b}$	10.1 (2, d, 162), 6.3 (2, d, 175), −10.1 (d, 134), −10.8 (d, 150), −11.9 (d, 168), −13.4 (d, 164), −23.3 (d, 164), −25.6 (d, 165), −27.9 (2, d, 165), −29.0 (d, 175), −30.1 (d, 171)
	$^1H^{a,c}$	6.53 (s, CH), 5.37 (s, CH), 5.04 (s, CH), 2.08 (s, Me), 1.92 (s, CH), 0.76 (s, Me)
6	$^{11}B^{b,f}$	9.2 (d, 158), 5.8 (d, 164), −3.1 (d, 155), −11.4 (d, 156), −27.2 (d, 162), −28.1 (d, 147), −30.4 (d, 165)
	$^1H^{c,f}$	6.15 (s, C3H), 2.69 (s, Me), 1.51 (s, C4H)
7	$^{11}B^{a,b}$	4.5 (d, 151), 1.4 (d, 161), −9.6 (d, 129), −10.3 (d, 132), −24.2 (d, 142), −27.4 (d, 156),−32.8 (d, 158)
	$^1H^{a,c}$	8.49 (Ph), 7.26 (Ph), 6.79 (Ph), 6.74 (s, C3H), 3.75 (s, Cp), 1.50 (s, C4H)
8	$^{11}B^{a,b}$	4.6 (d, 150), 2.8 (d, 191), −7.9 (2, d, 143), −27.5 (2, d, 144), −29.1 (d, 163)
	$^1H^{a,c}$	8.21 (Ph), 7.27 (Ph), 6.75 (Ph), 5.08 (s, C3H), 2.17 (s, C4H), 1.19 (s, Cp*)
9	$^{11}B^{a,b}$	8.9 (d, 150), 6.6 (d, 157), −5.1 (d, 152), −6.0 (d, 143), −21.1 (d, 146), −22.9 (d, 163), −30.5 (d, 158)
	$^1H^{a,c}$	6.78 (Ph), 6.23 (s, C3H), 4.68 (Ph), 4.53 (Ph), 4.49 (Ph), 4.31 (Ph), 3.67 (Cp), 1.41 (C4H)
10	$^{11}B^{b,f}$	−0.9 (d, 146), −3.5 (d, 140), −12.2 (d, 141), −13.3 (d, ∼150), −14.6 (d, 137), −20.4 (d, 148), −33.9 (d, 131)
	$^1H^{c,f}$	4.93 (br, s, C3H), 1.92 (s, Me), 1.70 (s, Bu^t), 1.67 (s, Cp*)
	$^{13}C^{d,e,f}$	94.91 (s, C_5Me_5), 94.54 (s, C3H), 66.24 (br, s, C2H), 38.11 (br, s, C4H), 32.19 (s, Me), 31.01 (CNC{Me_3}), 9.60 (s, C_5Me_5)
11	$^{11}B^{a,b}$	7.3 (d, 126), 4.4 (d, 144), 1.5 (d, 147), −6.1 (d, 140), −7.1 (d, 173), −12.1 (d, 140), −21.9 (d, 130)
	$^1H^{a,c}$	7.33 (Ph), 7.03 (Ph), 6.94 (Ph), 4.09 (s, Cp), 2.21 (br, s, C10H), 1.14 (Bu^t)
	$^{13}C^{a,d,e}$	155.57 (*C* NC{Me_3}), 126.26 (s, Ph), 83.37 (s, Cp), 81.32 (s, C3H), 53.92 (CN*C* {Me_3}), 30.62 (CNC{Me_3})

[a] In C_6D_6. [b] 160.5 MHz. [c] 500 MHz. [d] 125.8 MHz. [e] Broad-band decoupled. [f] In CD_2Cl_2.

High- and low-resolution mass spectra were obtained on a VG-ZAB-E high-resolution mass spectrometer. IR spectra were obtained on a Perkin-Elmer System 2000 FTIR spectrometer. Elemental analyses were done at the University of Pennsylvania microanalysis facility. Melting points were determined using a standard melting point apparatus and are uncorrected.

Electrochemical Procedures. Electrochemical procedures were generally as described previously[3g] and performed in either CH_2Cl_2 or THF containing 0.1 M $[NBu_4][B(C_6F_5)_4]$. The supporting electrolyte was prepared by metathesis of Li-$[B(C_6F_5)_4]$ etherate (Boulder Scientific Co.) with $[NBu_4]Br$ in methanol and recrystallized several times from CH_2Cl_2/OEt_2.[9] Although the experimental reference electrode was a Ag/AgCl

(3) (a) Plumb, C. A.; Carroll, P. J.; Sneddon, L. G. *Organometallics* **1992**, *11*, 1665−1671. (b) Plumb, C. A.; Carroll, P. J.; Sneddon, L. G. *Organometallics* **1992**, *11*, 1672−1680. (c) Barnum, B. A.; Carroll, P. J.; Sneddon, L. G. *Organometallics* **1996**, *15*, 645−654. (d) Weinmann, W.; Wolf, A.; Pritzkow, H.; Siebert, W.; Barnum, B. A.; Carroll, P. J.; Sneddon, L. G. *Organometallics* **1995**, *14*, 1911−1919. (e) Barnum, B. A.; Carroll, P. J.; Sneddon, L. G. *Inorg. Chem.* **1997**, *36*, 1327−1337. (f) Müller, T.; Kadlecek, D. E.; Carroll, P. J.; Sneddon, L. G.; Siebert, W. *J. Organomet. Chem.* **2000**, *614*−*615*, 125−130. (g) Wasczcak, M. D.; Wang, Y.; Garg, A.; Geiger, W. E.; Kang, S. O.; Carroll, P. J.; Sneddon, L. G. *J. Am. Chem. Soc.* **2001**, *123*, 2783−2790.

(4) Kang, S. O.; Furst, G. T.; Sneddon, L. G. *Inorg. Chem.* **1989**, *28*, 2339−2347.

(5) Ramachandran, B. M.; Carroll, P. J.; Sneddon, L. G. *J. Am. Chem. Soc.* **2000**, *122*, 11033−11034.

(6) For some examples see: (a) Basolo, F. *New J. Chem.* **1994**, *18*, 19−24, and references therein. (b) Basolo, F. *Polyhedron* **1990**, *9*, 1503−1535, and references therein. (c) O'Connor, J. M.; Casey, C. P. *Chem. Rev.* **1987**, *87*, 307−318, and references therein. (d) Schuster-Woldan, H. G.; Basolo, F. *J. Am. Chem. Soc.* **1966**, *88*, 1657−1663. (e) Rerek, M. E.; Basolo, F. *J. Am. Chem. Soc.* **1984**, *106*, 5908−5912. (f) Simanko, W.; Tesch, W.; Sapunov, V. N.; Mereiter, K.; Schmid, R.; Kirchner, K.; Coddington, J.; Wherland, S. *Organometallics* **1998**, *17*, 5674−5688. (g) Calhorda, M. J.; Gamelas, C. A.; Romão, C. C.; Veiros, L. F. *Eur. J. Inorg. Chem.* **2000**, 331−340.

(7) Shriver, D. F.; Drezdzon, M. A. *The Manipulation of Air-Sensitive Compounds*, 2nd ed.; Wiley: New York, 1986.

(8) Ramachandran, B. M.; Carroll, P. J.; Sneddon, L. G. In preparation.

Table 2. Crystallographic Data Collection and Structure Refinement Information

	4	**5**	**6**	**7**
formula	$RuC_8B_{14}H_{24}$	$OsC_8B_{14}H_{24}$	$OsC_8B_{14}H_{24}$	$FeC_{14}B_7H_{19}$
fw	372.68	461.81	461.81	318.81
cryst class	triclinic	triclinic	triclinic	triclinic
space group	$P\bar{1}$ (#2)	$P\bar{1}$ (#2)	$P\bar{1}$ (#2)	$P\bar{1}$ (#2)
Z	2	2	2	2
a, Å	6.6631(5)	10.706(3)	7.7980(6)	8.0188(3)
b, Å	7.7448(7)	12.373(3)	17.6859(11)	15.4779(7)
c, Å	17.686(2)	6.828(2)	6.6743(4)	6.7169(2)
α, deg	78.034(9)	92.45(2)	99.126(5)	97.413(2)
β, deg	80.883(9)	94.08(2)	109.228(4)	107.522(3)
γ, deg	71.114(8)	105.70(2)	78.123(4)	76.351(3)
V, Å^3	840.67(14)	866.7(4)	846.41(10)	771.02(5)
μ, cm^{-1}	9.13	73.38	75.14	9.62
cryst size, mm	0.25 × 0.20 × 0.15	0.42 × 0.24 × 0.04	0.30 × 0.11 x 0.02	0.35 × 0.30 × 0.14
D_{calc}, g/cm^3	1.472	1.770	1.812	1.373
F(000)	372	436	436	328
radiation	Mo Kα (λ = 0.71069 Å)	Mo Kα (λ = 0.71069 Å)	Mo Kα (λ = 0.71069 Å)	Mo Kα (λ = 0.71069 Å)
2θ range, deg	5.74−54.9	3.42−50.7	5.6−55.02	5.42−50.7
hkl collected	$-7 \le h \le 8$; $-7 \le k \le 9$; $-22 \le l \le 22$	$-12 \le h \le 12$; $-14 \le k \le 14$; $-7 \le l \le 8$	$-10 \le h \le 10$; $-22 \le k \le 21$; $-8 \le l \le 8$	$-9 \le h \le 9$; $-21 \le k \le 19$; $-12 \le l \le 11$
no. reflns measd	5439	4873	9073	6640
no. unique reflns	3199 (R_{int} = 0.0169)	2761 (R_{int} = 0.0417)	3539 (R_{int} = 0.0450)	2614 (R_{int} = 0.0247)
no. obsd reflns	2969 ($F>4\sigma$)	2386 ($F>4\sigma$)	3370 ($F>4\sigma$)	2482 ($F>4\sigma$)
no. reflns used in refinement	3199	2761	3539	2614
no. params	304	210	209	255
R indices ($F>4\sigma$)	R_1 = 0.0208 wR_2 = 0.0488	R_1 = 0.0784 wR_2 = 0.1709	R_1 = 0.0500 wR_2 = 0.1296	R_1 = 0.0407 wR_2 = 0.1066
R indices (all data)	R_1 = 0.0236 wR_2 = 0.0495	R_1 = 0.0904 wR_2 = 0.1818	R_1 = 0.0529 wR_2 = 0.1372	R_1 = 0.0433 wR_2 = 0.1105
GOF	1.017	1.123	1.073	1.040
final diff peaks, e/Å^3	+0.394, −0.867	+2.604, −2.413	+2.007, −2.472	+0.359, −0.524

	8	**9**	**10**	**11**
formula	$RuC_{19}B_7H_{29}$	$FeCrC_{17}B_7H_{19}O_3$	$RuC_{19}B_7H_{36}N$	$FeC_{19}B_7H_{28}N$
fw	434.16	454.84	455.23	401.94
cryst class	triclinic	monoclinic	triclinic	monoclinic
space group	$P\bar{1}$ (#2)	$P2_1/n$ (#14)	$P\bar{1}$ (#2)	$P2_1$ (#4)
Z	4	8	2	2
a, Å	14.8296(2)	14.6585(3)	9.9335(4)	10.5638(10)
b, Å	16.5710(1)	13.7293(3)	13.4379(4)	9.6335(5)
c, Å	9.7056(1)	20.0208(3)	9.6881(4)	11.0574(10)
α, deg	96.141(1)		104.997(3)	
β, deg	97.725(1)	102.640(1)	110.448(2)	113.370(3)
γ, deg	115.837(1)		76.334(3)	
V, Å^3	2090.20(4)	3931.55(13)	1155.16(7)	1033.0(2)
μ, cm^{-1}	7.51	13.07	6.83	7.34
cryst size, mm	0.36 × 0.22 × 0.06	0.22 × 0.20 × 0.008	0.40 × 0.20 × 0.07	0.15 × 0.12 × 0.10
D_{calc}, g/cm^3	1.380	1.537	1.309	1.292
F(000)	888	1840	472	420
radiation	Mo Kα (λ = 0.71069 Å)	Mo Kα (λ = 0.71069 Å)	Mo Kα (λ = 0.71069 Å)	Mo Kα (λ = 0.71069 Å)
2θ range, deg	5.04−54.96	5.12−50.7	5.02−50.7	5.84−50.7
hkl collected	$-19 \le h \le 19$; $-16 \le k \le 16$; $-23 \le l \le 24$	$-16 \le h \le 17$; $-16 \le k \le 16$; $-23 \le l \le 24$	$-11 \le h \le 11$; $-16 \le k \le 16$; $-11 \le l \le 11$	$-12 \le h \le 12$; $-11 \le k \le 11$; $-13 \le l \le 13$
no. reflns measd	21 788	28 993	9708	7727
no. unique reflns	8818 (R_{int} = 0.0506)	6890 (R_{int} = 0.0499)	3919 (R_{int} = 0.0506)	3564 (R_{int} = 0.0531)
no. obsd reflns	8202 ($F>4\sigma$)	6206 ($F>4\sigma$)	3755 ($F>4\sigma$)	3351 ($F>4\sigma$)
no. reflns used in refinement	8818	6890	3919	3564
no. params	561	595	290	254
R indices ($F>4\sigma$)	R_1 = 0.0439 wR_2 = 0.1066	R_1 = 0.0632 wR_2 = 0.1391	R_1 = 0.0577 wR_2 = 0.1562	R_1 = 0.0780 wR_2 = 0.2090
R indices (all data)	R_1 = 0.0480 wR_2 = 0.1105	R_1 = 0.0728 wR_2 = 0.1442	R_1 = 0.0594 wR_2 = 0.1583	R_1 = 0.0824 wR_2 = 0.2143
GOF	1.121	1.189	1.094	1.100
final diff peaks, e/Å^3	+0.587,−0.680	+0.305, −0.643	+0.855, −1.735	+1.380, −0.847

electrode, all potentials in this paper are referred to the ferrocene/ferrocenium potential, which was determined in each experiment at an appropriate point by using Cp_2Fe as an internal standard. Each process had diffusion-controlled behavior, and no electrode history problems were encountered at either glassy carbon or platinum electrodes (of 2 mm diameter). The potentiostat was a Princeton Applied Research Model 273 system interfaced to a personal computer. Standard

diagnostics[10] were applied to voltammetric responses, details of which are available elsewhere.[11] The following potentials of metallocene redox processes were used when comparing their potentials to the $E_{1/2}$ values of the tricarbadecaboranyl compounds: $Cp_2Fe^{+/0} = 0$; $Cp_2Fe^{0/1-} = -3.4$ V; $Cp_2Ru^{+/0} = 0.41$ V; $CpCp^*Ru^{+/0} = 0.11$ V; $Cp_2Ru^{0/1-} = -3.9$ V; $CpCp^*Ru^{0/1-} = -4.2$ V (estimated; not reported); $Cp_2Os^{+/0} = 0.25$ V; $Cp_2Os^{0/1-} = -3.9$ V (see Tables for literature sources).

1-(η^5-C_5Me_5)-2-Me-*closo*-1,2,3,4-$RuC_3B_7H_9$ (3). A toluene solution of $\mathbf{1}^-$ (1.5 mL of 0.5 M, 0.75 mmol) was added dropwise to a stirring solution of $[Cp^*RuCl_2]_x$ (0.11 g, 0.37 mmol) in glyme (35 mL). After stirring for 12 h at 50 °C, the dark brown solution was exposed to air and filtered. The solvent was vacuum evaporated from the filtrate to give a dark red residue, which was then extracted with Et_2O. TLC separation (7:3 hexanes/CH_2Cl_2) gave a single orange band (R_f 0.60). For **3**: 1-(η^5-C_5Me_5)-2-Me-*closo*-1,2,3,4-$RuC_3B_7H_9$, yield 75% (0.10 g, 0.28 mmol); orange, mp 211 °C. Anal. Calcd: C, 45.19, H, 7.31. Found: C, 44.91; H, 7.32. HRMS calcd for $^{12}C_{14}{}^1H_{27}{}^{11}B_7{}^{104}Ru$ *m/e* 376.1819, found 376.1840; IR (KBr, cm^{-1}) 2920 (m), 2571 (s), 1559 (w), 1472 (w), 1374 (w), 1028 (w), 967 (w), 790 (w), 727 (w), 668 (m).

***commo*-*Ru*-(2-Me-*closo*-1,2,3,4-$RuC_3B_7H_9)_2$ (4).** A toluene solution of $\mathbf{1}^-$ (2.04 mL of 0.5 M, 1.02 mmol) was added dropwise to a stirring solution of $[RuCl_2(cod)_x]$ (0.14 g, 0.51 mmol) in glyme (35 mL). After stirring for 12 h at reflux, the red solution was exposed to air and filtered through a silica gel plug. The silica gel was washed with diethyl ether to extract any product. TLC separation (9:1 hexanes/toluene) gave three bands with only the third dark red band (R_f 0.2) obtained in sufficient amount for complete characterization. For **4**: *commo*-*Ru*-(2-Me-*closo*-1,2,3,4-$RuC_3B_7H_9)_2$, yield 8% (0.02 g, 0.04 mmol); red; mp 110 °C. Anal. Calcd: C, 25.78, H, 6.49. Found: C, 26.28, H, 6.58. HRMS calcd for $^{12}C_8{}^1H_{24}{}^{11}B_{14}{}^{104}Ru$ 378.2236. Found: 378.2220. IR (KBr, cm^{-1}) 3027 (s), 2998 (m), 2938 (s), 2861 (m), 2573 (s), 1852 (w), 1439 (s), 1376 (s), 1276 (m), 1099 (s), 967 (s), 931 (m), 865 (m), 838 (m), 791 (m), 725 (w), 696 (m), 645 (w).

***commo*-*Os*-(4′-Me-*closo*-1′,2′,3′,4′-$OsC_3B_7H_9$)(2-Me-*closo*-1,2,3,4-$OsC_3B_7H_9$) (5) and *commo*-*Os*-(2-Me-*closo*-1,2,3,4-$OsC_3B_7H_9)_2$ (6).** A toluene solution of $\mathbf{1}^-$ (2.68 mL of 0.5 M, 1.34 mmol) was added dropwise to a stirring solution of $Na_2OsCl_6{\cdot}4H_2O$ (0.30 g, 0.67 mmol) in glyme (35 mL). After stirring for 12 h at reflux, the reddish-brown solution was exposed to air and filtered through a silica gel plug. The silica gel was washed with CH_2Cl_2 to extract any product. TLC separation (9:1 hexanes/toluene) gave two bands (overall yield 7.7%, 0.024 g, 0.05 mmol). For **5**: *commo*-*Os*-(4′-Me-*closo*-1′,2′,3′,4′-$OsC_3B_7H_9$)(2-Me-*closo*-1,2,3,4-$OsC_3B_7H_9$), (R_f 0.3), yield 2.3% (0.007 g); orange; mp 160 °C. Anal. Calcd: C, 20.81, H, 5.24. Found: C, 20.58, H, 5.17. HRMS calcd for $^{12}C_8{}^1H_{24}{}^{11}B_{14}{}^{192}Os$ 466.2793, found 466.2815; IR (KBr, cm^{-1}) 3038 (m), 2937 (m), 2578 (s), 1477 (m), 1386 (m), 1276 (m), 1160 (w), 1102 (m), 921 (m), 720 (w), 668 (s), 649 (w). For **6**: *commo*-*Os*-(2-Me-*closo*-1,2,3,4-$OsC_3B_7H_9)_2$ (R_f 0.2); yield 5.4% (0.017 g); orange; mp 162 °C. Anal. Calcd: C, 20.81, H, 5.24. Found: C, 21.04, H, 5.42. HRMS calcd for $^{12}C_8{}^1H_{24}{}^{11}B_{14}{}^{192}Os$ 466.2793, found 466.2815; IR (KBr, cm^{-1}) 3031 (m), 2570 (s), 1413 (w), 1329 (w), 1160 (m), 1102 (m), 921 (s), 756 (w).

1-(η^5-C_5H_5)-2-Ph-*closo*-1,2,3,4-$FeC_3B_7H_9$ (7). A toluene solution of $\mathbf{2}^-$ (2.2 mL of 0.5 M, 1.10 mmol) was added dropwise to a stirring solution of (η^5-C_5H_5)Fe(CO)$_2$I (0.304 g, 1.00 mmol) in THF (35 mL). After stirring for 12 h at room temperature, the bluish-green solution was exposed to air and filtered through a silica gel plug, and the dark filtrate was evaporated to dryness. TLC separation (7:3 hexanes/CH_2Cl_2) gave a dark blue band (R_f 0.55). For **7**: 1-(η^5-C_5H_5)-2-Ph-*closo*-1,2,3,4-$FeC_3B_7H_9$, yield 49% (0.156 g, 0.49 mmol); dark blue; mp 150 °C. Anal. Calcd: C, 52.74; H, 6.01. Found: C, 52.47; H, 5.78. HRMS calcd for $^{12}C_{14}{}^1H_{19}{}^{11}B_7{}^{56}Fe$ 320.1487, found 320.1507; IR (KBr, cm^{-1}) 3110 (m), 3063 (m), 2552 (s), 1419 (m), 1308 (m), 1260 (m), 1199 (m), 1116 (w), 939 (w), 838 (w), 738 (w), 668 (s).

1-(η^5-C_5Me_5)-2-Ph-*closo*-1,2,3,4-$RuC_3B_7H_9$ (8). A toluene solution of $\mathbf{2}^-$ (1.6 mL of 0.5 M, 0.80 mmol) was added dropwise to a stirring solution of $[Cp^*RuCl_2]_x$ (0.12 g, 0.39 mmol) in glyme (35 mL). After stirring for 12 h at 50 °C, the yellow-orange solution was exposed to air and filtered through a silica gel plug. The silica gel was washed with Et_2O to extract any remaining product. TLC separation (7:3 hexanes/CH_2Cl_2) gave a single orange band (R_f 0.55). For **8**: 1-(η^5-C_5Me_5)-2-Ph-*closo*-1,2,3,4-$RuC_3B_7H_9$, yield 66% (0.112 g, 0.26 mmol); orange; mp 179 °C. Anal. Calcd: C, 52.56, H, 6.73. Found: C, 53.29, H, 6.87. HRMS calcd for $^{12}C_{19}{}^1H_{29}{}^{11}B_7{}^{104}Ru$ 438.1976, found 438.1991; IR (KBr, cm^{-1}) 2921 (s), 2546 (s), 1945 (m), 1494 (w), 1374 (w), 1160 (w), 1102 (m), 929 (m), 691 (m), 668 (s).

Reaction of $\mathbf{2}^-$ with $[RuCl_2(cod)_x]$. A toluene solution of $\mathbf{2}^-$ (2.04 mL of 0.5 M, 1.02 mmol) was added dropwise to a stirring solution of $[RuCl_2(cod)_x]$ (0.143 g, 0.51 mmol) in glyme (35 mL). After stirring for 12 h at reflux, the resulting dark brown solution was worked up as reported above for the reaction of $\mathbf{1}^-$ with $[RuCl_2(cod)_x]$, but yielded no isolable products.

Reaction of 7 with $Cr(CO)_6$: Synthesis of 1-(η^5-C_5H_5)-2-[(η^6-C_6H_5)Cr(CO)$_3$]-*closo*-1,2,3,4-$FeC_3B_7H_9$ (9). A 0.63 mmol (0.202 g) sample of **7** was dissolved in a 10:1 mixture of dibutyl ether/THF, and then an excess (1.39 g, 6.3 mmol) of $Cr(CO)_6$ was added. After reflux for 36 h, the volatiles were vacuum evaporated. TLC separation (CH_2Cl_2) gave a blue band of the unreacted starting compound **7** (R_f 0.8) (0.074 g, 0.23 mmol, 37%) and a green band (R_f 0.5) of the product. For **9**: 1-(η^5-C_5H_5)-2-[(η^6-C_6H_5)Cr(CO)$_3$]-*closo*-1,2,3,4-$FeC_3B_7H_9$; yield 12% (0.023 g, 0.05 mmol); green; mp 150 °C. Anal. Calcd: C, 44.89; H, 4.21. Found: C, 43.19; H, 4.67. HRMS calcd for $^{12}C_{17}{}^1H_{19}{}^{11}B_7{}^{52}Cr{}^{56}Fe{}^{16}O_3$ 456.0740, found 456.0749; IR (KBr, cm^{-1}) 3118 (s), 3067 (s), 3044 (m), 2633 (s), 2563 (s), 2504 (s), 2491 (s), 1965 (s), 1894 (s), 1872 (s), 1521 (m), 1504 (m), 1452 (s), 1425 (s), 1407 (m), 1363 (w), 1299 (m), 1216 (s), 1119 (s), 1060 (w), 1012 (m), 995 (m), 850 (s), 814 (m), 731 (m).

Reaction of 3 with *tert*-Butylisocyanide: Synthesis of 8-(η^5-C_5Me_5)-8-(CNBu^t)-9-Me-*nido*-8,7,9,10-$RuC_3B_7H_9$ (10). A 0.03 mmol (0.011 g) sample of **3** was dissolved in ~3 mL of glyme, and excess (1.0 mL, 8.9 mmol) *tert*-butylisocyanide was added. An immediate color change from reddish-orange to yellow was observed. Slow evaporation of the solution gave X-ray quality yellow-colored crystals. For **10**: *nido*-8-(η^5-C_5Me_5)-8-(CNBu^t)-9-Me-*nido*-8,7,9,10-$RuC_3B_7H_9$; yield 97% (0.013 g, 0.029 mmol); orange. Anal. Calcd: C, 50.13; H, 7.97; N, 3.08. Found: C, 49.98; H, 8.14; N, 2.74. IR (KBr, cm^{-1}) 3014 (s), 2983 (s), 2911 (s), 2855 (s), 2527(s), 2163 (s), 2069 (s), 1856 (m), 1460 (s), 1377 (s), 1259 (m), 1232 (s), 1085 (s), 1048 (s), 971 (s), 951 (m), 928 (w), 886 (m).

Reaction of 7 with *tert*-Butylisocyanide: Synthesis of 8-(η^5-C_5H_5)-8-(CNBu^t)-9-Ph-*nido*-8,7,9,10-$FeC_3B_7H_9$ (11). A 0.03 mmol (0.010 g) sample of **7** was dissolved in ~3 mL of toluene, and excess (1.0 mL, 8.9 mmol) *tert*-butylisocyanide was added. An immediate color change from blue-green to brownish-red was observed. X-ray quality brownish-red colored crystals were obtained by cooling the brownish-red solution at 0 °C. For **11**: 8-(η^5-C_5H_5)-8-(CNBu^t)-9-Ph-*nido*-8,7,9,10-$FeC_3B_7H_9$; yield 63% (0.008 g, 0.019 mmol); brownish-red. Anal. Calcd: C, 56.77; H, 7.02; N, 3.48. Found: C, 56.17; H, 7.06; N, 3.54. IR (KBr, cm^{-1}) 3110 (s), 3087 (s), 2985 (s), 2870 (m), 2555 (s), 2166 (s), 2048 (m), 1961 (m), 1862 (m), 1494 (s), 1445 (s), 1370 (s), 1232 (w), 1199 (s), 1068 (m), 939 (s), 894 (m), 839 (s).

(9) LeSuer, R. J.; Geiger, W. E. *Angew. Chem., Int. Ed.* **2000**, *39*, 248−250.
(10) Geiger, W. E., Kissinger, P. T., Heineman, W. R., Eds. *Laboratory Techniques In Electroanalytical Chemistry*, 2nd ed.; Marcel Dekker: New York, 1996; Chapter 23.
(11) Trupia, S. M. Ph.D. Thesis, University of Vermont, 2002.

Reaction of 4 with *tert*-Butylisocyanide. A 0.03 mmol (0.011 g) sample of **4** was dissolved in ~3 mL of glyme, and excess (1.0 mL, 8.9 mmol) *tert*-butylisocyanide was added. No color change was observed, and there was no change in the ^{11}B NMR spectrum from that of the starting compound.

Crystallographic Data. Single crystals of all compounds were grown via slow solvent evaporation from dichloromethane or a 50:50 hexanes/dichloromethane solutions in air.

Collection and Reduction of the Data. Crystallographic data and structure refinement information are summarized in Table 2. X-ray intensity data were collected on a Rigaku R-axis IIc area detector employing graphite-monochromated Mo Kα radiation at a temperature of 210 K. Indexing was performed from a series of oscillation angles. A hemisphere of data was collected using 0.5° oscillation angles for **4**, 10° for **5** and **7**, 5° for **6**, **9**, and **11**, 4° for **8**, and 6° for **10** and a crystal-to-detector distance of 82 mm. Oscillation images were processed using bioteX,[12] producing a listing of unaveraged F and $\sigma(F)$ values that were then passed to the teXsan program package[13] for further processing and structure solution on a Silicon Graphics Indigo R4000 computer. The intensity data were corrected for Lorentz and polarization effects but not for absorption.

Solution and Refinement of the Structures. The structures were solved by direct methods (SIR92).[14] Refinements were by full-matrix least squares based on F^2 using SHELXL-93.[15] All reflections were used during refinement (values of F^2 that were experimentally negative were replaced by $F^2 = 0$).

Results and Discussion

Syntheses and Structural Characterizations. As illustrated in eq 1, we have previously shown[3a,b] that ferratricarbadecaboranyl analogues of ferrocene, including both bis-cage (Me-$C_3B_7H_9$)$_2$Fe and mixed-ligand (η^5-C_5H_5)Fe(Me-$C_3B_7H_9$) complexes, can be prepared by the reactions of the 6-Me-*nido*-5,6,9-$C_3B_7H_9^-$ (**1**$^-$) anion with (η^5-C_5H_5)Fe(CO)$_2$I.

(η^5-C_5H_5)Fe(CO)$_2$I + Li$^+$(6-Me-*nido*-5,6,9-$C_3B_7H_9$)$^-$ → (**1**$^-$) 1-(η^5-C_5H_5)-2-Me-*closo*-1,2,3,4-Fe$C_3B_7H_9$ + (**12**) 1-(η^5-C_5H_5)-4-Me-*closo*-1,2,3,4-Fe$C_3B_7H_9$ + (**13**) *commo-Fe*-(5-Me-*closo*-1,2,3,5-$C_3B_7H_9$)(4-Me-*closo*-1,2,3,4-$C_3B_7H_9$) + (**14**) LiI + 2CO (1)

We have now used the reactions given in eqs 2−4 to prepare methyltricarbadecaboranyl analogues of ruthenocene and osmocene.

[(η^5-C_5Me_5)RuCl$_2$]$_x$ + 2Li$^+$(6-Me-*nido*-5,6,9-$C_3B_7H_9$)$^-$ → (**1**$^-$) 1-(η^5-C_5Me_5)-2-Me-*closo*-1,2,3,4-Ru$C_3B_7H_9$ + (**3**) 2LiCl (2)

[RuCl$_2$(cod)$_x$] + 2Li$^+$(6-Me-*nido*-5,6,9-$C_3B_7H_9$)$^-$ → (**1**$^-$) *commo-Ru*-(2-Me-*closo*-1,2,3,4-Ru$C_3B_7H_9$)$_2$ + (**4**) 2LiCl (3)

Na$_2$OsCl$_6$·4H$_2$O + 4Li$^+$(6-Me-*nido*-5,6,9-$C_3B_7H_9$)$^-$ → *commo-Os*-(4′-Me-*closo*-1′,2′,3′,4′-Os$C_3B_7H_9$)(2-Me-*closo*-1,2,3,4-Os$C_3B_7H_9$) + (**5**) *commo-Os*-(2-Me-*closo*-1,2,3,4-Os$C_3B_7H_9$)$_2$ + (**6**) 2NaCl + 4LiCl + 4H$_2$O (4)

Likewise, the syntheses of the phenyltricarbadecaboranyl analogues of ferrocene and ruthenocene were achieved by the reactions given in eqs 5 and 6 employing the new 6-Ph-*nido*-5,6,9-$C_3B_7H_9^-$ anion.[8]

(η^5-C_5H_5)Fe(CO$_2$)I + Li$^+$(6-Ph-*nido*-5,6,9-$C_3B_7H_9$)$^-$ → (**2**$^-$) 1-(η^5-C_5H_5)-2-Ph-*closo*-1,2,3,4-Fe$C_3B_7H_9$ + LiI + (**7**) 2CO (5)

[(η^5-C_5Me_5)RuCl$_2$]$_x$ + 2Li$^+$(6-Ph-*nido*-5,6,9-$C_3B_7H_9$)$^-$ → (**2**$^-$) 1-(η^5-C_5Me_5)-2-Ph-*closo*-1,2,3,4-Ru$C_3B_7H_9$ + (**8**) 2LiCl (6)

Significant differences were observed in the reactions employing the 6-Me-*nido*-5,6,9-$C_3B_7H_9^-$ (**1**$^-$) and 6-Ph-*nido*-5,6,9-$C_3B_7H_9^-$ (**2**$^-$) anions. For example, 6-Me-*nido*-5,6,9-$C_3B_7H_9^-$ reactions usually result in some cage-carbon rearrangement to produce isomeric side products, such as the 1-(η^5-C_5H_5)-4-Me-*closo*-1,2,3,4-Fe$C_3B_7H_9$ (**13**) complex in eq 1, in which "methyl-migration" to the 4-cage carbon has occurred.[16] However, in comparable reactions employing the 6-Ph-*nido*-5,6,9-$C_3B_7H_9^-$ anion, no such isomerization occurs and only one isomer is produced. Likewise, in 6-Me-*nido*-5,6,9-$C_3B_7H_9^-$ reactions such as in eq 1, bis-cage, (Me-$C_3B_7H_9$)$_2$M, side products are usually produced (for example, complex **14**), but in the 6-Ph-*nido*-5,6,9-$C_3B_7H_9^-$ reactions in eqs 5 and 6, no bis-cage (Ph-$C_3B_7H_9$)$_2$M, M = Fe or Ru, were observed. In fact, even reactions, such as shown in eq 7, intentionally designed to produce bis-cage complexes

(12) *bioteX*: A suite of Programs for the Collection, Reduction and Interpretation of Imaging Plate Data; Molecular Structure Corporation, 1995.

(13) *teXsan*: Crystal Structure Analysis Package; Molecular Structure Corporation, 1985 & 1992.

(14) *SIR92*: Altomare, A.; Burla, M. C.; Camalli, M.; Cascarano, M.; Giacovazzo, C.; Guagliardi, A.; Polidoro, G. *J. Appl. Crystallogr.* **1994**, *27*, 435.

(15) Sheldrick, G. M. *SHELXL-93*: Program for the Refinement of Crystal Structures; University of Göttingen: Germany, 1993.

(16) Plumb, C. A.; Sneddon, L. G. *Organometallics* **1992**, *11*, 1681−1685.

from the 6-Ph-*nido*-5,6,9-$C_3B_7H_9^-$ anion were unsuccessful.

$$[RuCl_2(cod)_x] + 2Li^+(\text{6-Ph-}\textit{nido}\text{-5,6,9-}C_3B_7H_9)^- \rightarrow \text{no reaction} \quad (7)$$
$$\mathbf{2}^-$$

The inability to form bis-cage complexes containing the 6-Ph-*nido*-5,6,9-$C_3B_7H_9^-$ ligand is most probably a result of the unfavorable steric interactions between the phenyl substituents of the two cages. As will be reported elsewhere,[8] we have used this feature to advantage in achieving the high yield syntheses of a series of half-sandwich complexes that were unattainable using the 6-Me-*nido*-5,6,9-$C_3B_7H_9^-$ anion. The absence of both cage-isomerization and bis-cage side products in the reactions with the 6-Ph-*nido*-5,6,9-$C_3B_7H_9^-$ results in these reactions being more selective than the corresponding reactions with 6-Me-*nido*-5,6,9-$C_3B_7H_9^-$. Thus, reactions with the 6-Ph-*nido*-5,6,9-$C_3B_7H_9^-$ anion provide a more efficient route to metallatricarbadecaboranyl complexes than those reactions employing the 6-Me-*nido*-5,6,9-$C_3B_7H_9^-$ anion.

All complexes resulting from the reactions in eqs 1−6 were isolated as air-stable solids and were easily purified by TLC. The compositions of all compounds were established by mass spectrometry and/or elemental analyses. The proposed structures are strongly supported by their NMR data, with the structures of compounds **4**, **5**, **6**, **7**, and **8** being further confirmed by crystallographic determinations.

The ^{11}B NMR spectra (Table 1) of the mixed-ligand complexes, 1-(η^5-C_5Me_5)-2-Me-*closo*-1,2,3,4-$RuC_3B_7H_9$ (**3**), 1-(η^5-C_5H_5)-2-Ph-*closo*-1,2,3,4-$FeC_3B_7H_9$ (**7**), and 1-(η^5-C_5Me_5)-2-Ph-*closo*-1,2,3,4-$RuC_3B_7H_9$ (**8**), are each consistent with C_1 cage symmetries and are very similar to that previously reported for 1-(η^5-C_5H_5)-2-Me-*closo*-1,2,3,4-$FeC_3B_7H_9$ (**12**).[3a] The ^1H NMR spectra for compounds **3**, **7**, and **8** are likewise similar to that of **12**, each showing, in addition to the appropriate Me or Ph resonances, two C−H resonances with one occurring at a low-field shift (~6.8 to 4.8 ppm) characteristic of the proton attached to the low-coordinate C3 carbon, which is adjacent to the metal, and the other at a high-field shift (>2.2 ppm) characteristic of the C4-H proton.

In agreement with the spectroscopic data, the crystallographic determinations of 1-(η^5-C_5H_5)-2-Ph-*closo*-1,2,3,4-$FeC_3B_7H_9$ (**7**) (Figure 2) and 1-(η^5-C_5Me_5)-2-Ph-*closo*-1,2,3,4-$RuC_3B_7H_9$ (**8**) (Figure 3) confirm that the metal atoms in these complexes, as in **12**, are η^6-coordinated to the puckered six-membered face of the tricarbadecaboranyl cage with the Me or Ph groups bonded to the C2 cage carbon adjacent to the metal. Thus, these complexes, as well as **12** and 1-(η^5-C_5Me_5)-2-Me-*closo*-1,2,3,4-$RuC_3B_7H_9$ (**3**), can be considered as mixed ligand analogues of ferrocene and ruthenocene in which formal Fe^{2+} and Ru^{2+} ions are sandwiched between the tricarbadecaboranyl and cyclopentadienyl monoanionic ligands. From a cluster point of view,[17] the 11-vertex $MC_3B_7H_9$ fragment has a *closo* skeletal electron count (24 skeletal electrons, with the CpFe and Cp*Ru groups each donating 1 skeletal electron), and it therefore adopts the octadecahedral structure normally observed for such systems.

Selected bond distances for **12**, **7**, **8**, and **9** are compared in Table 3. The metals are approximately centered over the puckered six-membered open face, with the closest metal−cage interactions being with the

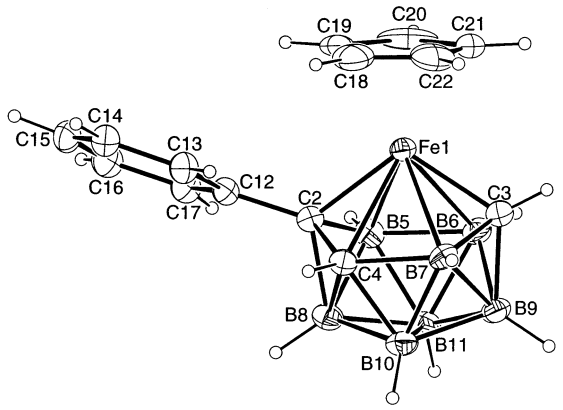

Figure 2. ORTEP drawing of the structure of 1-(η^5-C_5H_5)-2-Ph-*closo*-1,2,3,4-$FeC_3B_7H_9$ (**7**).

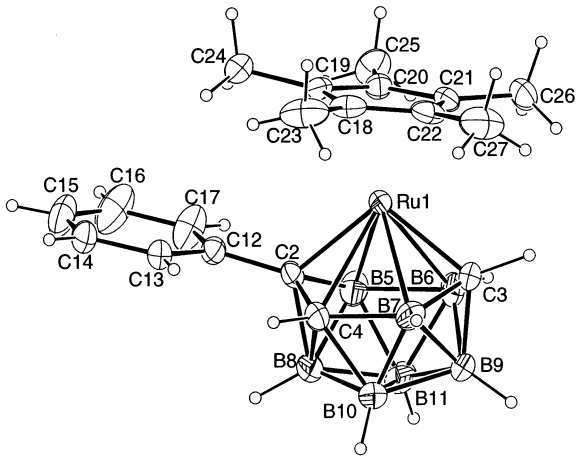

Figure 3. ORTEP drawing of the structure of 1-(η^5-C_5Me_5)-2-Ph-*closo*-1,2,3,4-$RuC_3B_7H_9$ (**8**).

Table 3. Intramolecular Distances (Å) in Compounds 12, 7, 8, and 9 (M = Fe for 12, 7, 9 and M = Ru for 8)

bond	**12**	**7**	**8**[a]	**9**[a]
M−C2	1.970(3)	1.982(3)	2.111(3)	1.980(4)
M−C3	1.951(3)	1.955(3)	2.073(4)	1.952(5)
M−C4	2.227(3)	2.258(3)	2.355(4)	2.274(5)
M−B5	2.264(3)	2.239(3)	2.339(5)	2.217(5)
M−B6	2.276(3)	2.253(3)	2.352(5)	2.230(6)
M−B7	2.241(3)	2.275(3)	2.358(4)	2.285(6)
M−Cp/Cp*	1.681	1.695(3)	1.829(2)	1.684(5)
C2−C4	1.560(4)	1.502(4)	1.509(6)	1.496(6)
C4−B7	1.817(5)	1.750(4)	1.781(7)	1.739(7)
B7−C3	1.564(4)	1.576(4)	1.570(7)	1.557(9)
C3−B6	1.574(4)	1.578(4)	1.578(8)	1.588(9)
B6−B5	1.775(5)	1.841(5)	1.833(7)	1.854(8)
B5−C2	1.508(3)	1.593(4)	1.577(6)	1.597(7)

[a] The bond distances of only one of the two independent molecules found in the asymmetric units of **8** and **9** are given, as there were no significant differences.

(17) (a) Wade, K. *Adv. Inorg. Chem. Radiochem.* **1976**, *18*, 1−66. (b) Williams, R. E. *Adv. Inorg. Chem. Radiochem.* **1976**, *18*, 67−142. (c) Williams, R. E. *Chem. Rev.* **1992**, *92*, 117−201. (d) Williams, R. E. In *Electron Deficient Boron and Carbon Clusters*; Olah, G. A., Wade, K., Williams, R. E., Eds.; Wiley: New York, 1991.

two carbons, C2 and C3, which are puckered out of the ring. Longer and approximately equivalent bond lengths are observed between the metals and the remaining four atoms (C4, B5, B6, and B7) on the tricarbadecaboranyl bonding face. The M−C2 and M−C3 bond lengths in **7** and **8** are significantly shorter than the M−C bond lengths found to the ring-carbons in their respective cyclopentadienyl (2.051(5)−2.069(3) Å) and pentamethylcyclopentadienyl (2.158(4)−2.261(2) Å) ligands. As pointed out previously,[18] the orbitals on the open face of even a planar polyhedral cluster are orientated more directly toward the metal than in a cyclopentadienyl ring. This enhances the overlap of the metal and ligand orbitals and strengthens the bonding. In the case of the tricarbadecaboranes, even stronger interactions could be possible because the puckered ring structure allows close approach of the metal to the C2 and C3 carbons.

Regardless of whether the substituent at the C2 carbon is a methyl or phenyl group, the M−C2 distance is found to be considerably lengthened compared to the M−C3 distance. For example, the Fe−C2 distances in **12** (1.970(3) Å) and **7** (1.982(3) Å) are considerably longer than their corresponding Fe−C3 distances (1.951-(3) and 1.955(3) Å, respectively).

The ^{11}B and ^{1}H NMR spectra (Table 1) of the bis-cage complexes *commo-Ru*-(2-Me-*closo*-1,2,3,4-$RuC_3B_7H_9)_2$ (**4**) and *commo-Os*-(2-Me-*closo*-1,2,3,4-$OsC_3B_7H_9)_2$ (**6**) are similar to those found for complexes **3**, **7**, **8**, and **12**, indicating that the two cages in **4** and **6** are equivalent. Thus, both complexes show only seven equal intensity doublets in their ^{11}B NMR spectra. Likewise, in their ^{1}H NMR spectra, the complexes show only a single Me resonance, as well as only two C-H resonances, one in the low-field region (6.05 ppm, **4** and 6.15 ppm, **6**) characteristic of a C3-H proton and the other at high-field (1.73 ppm, **4** and 1.51 ppm, **6**) consistent with a C4-H proton.[3]

The ^{11}B and ^{1}H NMR spectra of *commo-Os*-(4′-Me-*closo*-1′,2′,3′,4′-$OsC_3B_7H_9$)(2-Me-*closo*-1,2,3,4-$OsC_3B_7H_9$) (**5**) are much more complex, indicating that the two cages of the complex are not equivalent. Thus, the ^{11}B NMR resolves 14 resonances in 2:2:1:1:1:1:1:1:2:1:1 ratios. The ^{1}H NMR spectrum shows two separate methyl resonances (one at low field, 2.08 ppm, and the other at high field, 0.76 ppm), as well as three C-H resonances at low field (6.53, 5.37, and 5.04 ppm) and only one C-H at high field (1.92 ppm). The fact that in the ^{1}H NMR spectrum there are three low-field resonances (C2-H and C3-H adjacent to the metal) and only one high-field resonance (C4-H) suggests that a methyl group has migrated from the C2 to the C4 position on one of the two cages.[16]

As shown in Figures 4, 5, and 6, the structures of compounds **4**, **6**, and **5** were confirmed by crystallographic determinations and are in agreement with the spectroscopic data discussed above. The complexes can be considered analogues of ruthenocene and osmocene in which the Ru^{2+} and Os^{2+} ions are sandwiched between the two Me-$C_3B_7H_9^-$ monoanions. From a cluster point of view,[17] a (Me-$C_3B_7H_9$)M (M = Ru or Os)

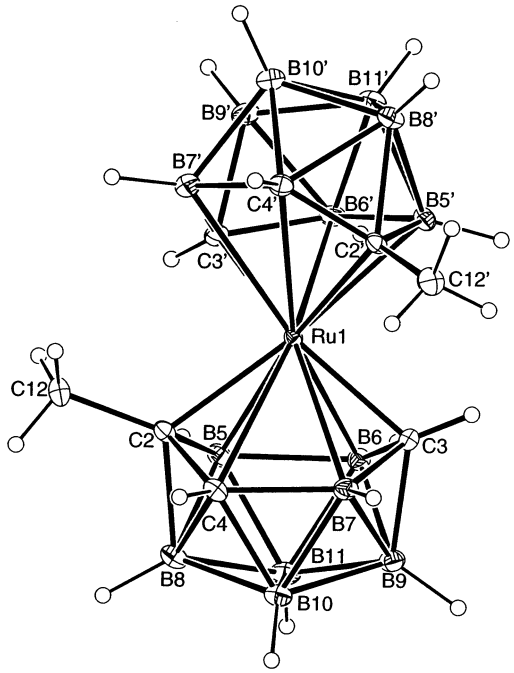

Figure 4. ORTEP drawing of the structure of *commo-Ru*-(2-Me-*closo*-1,2,3,4-$RuC_3B_7H_9)_2$ (**4**).

fragment, like the (η^5-C_5Me_5)M and (η^5-C_5H_5)M (M = Fe, Ru) groups in complexes **7** and **8**, can donate one skeletal electron to the second $MeC_3B_7H_9$ cage. Therefore, each ($MeC_3B_7H_9$)M unit would be an 11-vertex, 24-skeletal-electron system that should adopt the observed *closo*-octadecahedral geometry in which the metal is shared between the two cages.

As discussed[3b] previously, due to the fact that the 6-Me-*nido*-5,6,9-$C_3B_7H_9^-$ anion exists as a racemic mixture, when a bis-cage complex is formed, it may contain two anion cages of the same enantiomeric type or contain two different enantiomeric forms of the anion. As can be seen in Figures 4 and 5, both complexes **4** and **6** contain a single enantiomeric form of the 6-Me-*nido*-5,6,9-$C_3B_7H_9^-$ anion, and thus the two cages are related by a C_2-axis passing through the metal center. The symmetry equivalence of the two cages thus results in the simple NMR spectra observed for **4** and **6**. As can be seen in Figure 6, the structure of compound **5** is more complex since the two cages are not symmetry equivalent. Thus, the complex, unlike in **4** and **6**, contains two different enantiomeric forms of the anion. Furthermore, in one of the cages (the top cage in Figure 6) the methyl group that had originally been present at the C2′ carbon has rearranged to the C4′ carbon position. The inequivalence of the two cages, as well as the observed methyl rearrangement, is thus in complete accord with the NMR data.

Selected bond distances for **4**, **6**, and **5** are presented in Table 4. The metal ions are approximately centered over the six-membered, puckered open faces of the two cages. As was the case for complexes **7**, **8**, and **12**, the shortest metal−cage distances are between the metals and the two carbons, C2 and C3, puckered out of the six-membered face. While, as in the recently reported bis-cage vanadatricarbaboranyl complexes,[3g] the planes containing the three boron and one carbon (B5−B6−B7−C4) atom on the six-membered open faces of each

(18) (a) Hawthorne, M. F.; Young, D. C.; Andrews, T. D.; Howe, D. V.; Pilling, R. L.; Pitts, A. D.; Reintjes, M.; Warren, Jr., L. F.; Wegner, P. A. *J. Am. Chem. Soc.* **1968**, *90*, 879−896. (b) Calhorda, M. J.; Mingos, D. M. P.; Welch, A. *J. Organomet. Chem.* **1982**, *228*, 309−320. (c) Mingos, D. M. P. *J. Chem. Soc., Chem. Commun.* **1977**, 602−610.

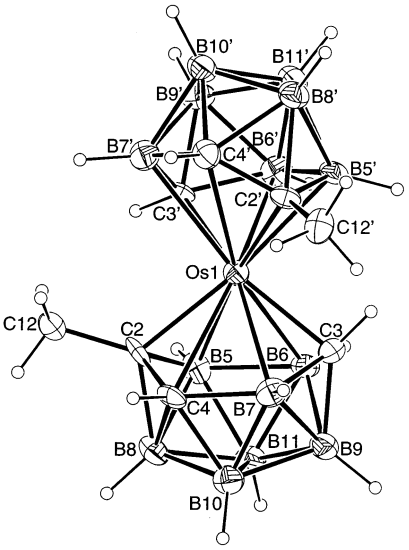

Figure 5. ORTEP drawing of the structure of *commo-Os*-(2-Me-*closo*-1,2,3,4-$OsC_3B_7H_9)_2$ (**6**).

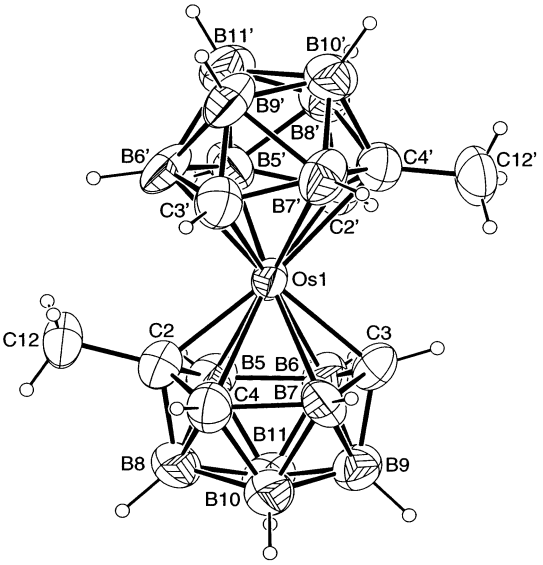

Figure 6. ORTEP drawing of the structure of *commo-Os*-(4′-Me-*closo*-1′,2′,3′,4′-$OsC_3B_7H_9$)(2-Me-*closo*-1,2,3,4-$OsC_3B_7H_9$) (**5**).

of the two cages of complex **5** are reasonably parallel (dihedral angle 6(3)°), those in **4** (dihedral angle 17.1(2)°) and **6** (dihedral angle 15.8(8)°) are not and are tilted away from each other on the C2-Me side of the cages. Unlike in the vanadatricarbaborane complexes, the two cages in **4**, **6**, and **5** are not aligned ~90° to one another: **4**, 50.48(7)°; **6**, 49.8(2)°; and **5**, 57.6(5)° (as measured by the dihedral angle between the C2−C3−B8−B9 and C2′−C3′−B8′−B9′ planes).

As noted earlier, the use of the 6-Ph-*nido*-5,6,9-$C_3B_7H_9^-$ anion has a number of advantages over the 6-Me-*nido*-5,6,9-$C_3B_7H_9^-$ anion in terms of both higher selectivity and yield of metallatricarbadecaboranyl products. The introduction of the phenyl substituent also provides a new reactive site for further modification of a complex. Indeed, as shown in eq 8, it was found that the phenyl-coordinated complex 1-(η^5-C_5H_5)-2-[(η^6-C_6H_5)-$Cr(CO)_3$]-*closo*-1,2,3,4-$FeC_3B_7H_9$ (**9**) was readily obtained by refluxing a mixture of **7** and $Cr(CO)_6$ in the mixed 10:1 dibutyl ether/THF solvent system which has been employed in the synthesis of (η^6-C_6H_6)$Cr(CO)_3$.[19,20]

Table 4. Intramolecular Distances (Å) in Compounds 4, 5, and 6 (M = Ru for 4 and Os for 5 and 6)

bond	4	5	6
M−C2	2.120(2)	2.14(2)	2.121(7)
M−C2′	2.116(2)	2.06(2)	2.114(7)
M−C3	2.053(2)	2.12(2)	2.078(8)
M−C3′	2.060(2)	2.09(2)	2.075(8)
M−C4	2.499(2)	2.45(2)	2.479(8)
M−C4′	2.494(2)	2.43(2)	2.478(9)
M−B5	2.349(2)	2.33(2)	2.333(11)
M−B5′	2.354(2)	2.24(3)	2.332(10)
M−B6	2.307(2)	2.37(3)	2.287(9)
M−B6′	2.296(2)	2.35(2)	2.313(10)
M−B7	2.458(2)	2.43(3)	2.459(11)
M−B7′	2.467(2)	2.42(3)	2.469(11)
C2−C4	1.491(3)	1.51(3)	1.517(13)
C2′−C4′	1.494(3)	1.46(3)	1.501(12)
C4−B7	1.747(3)	1.74(3)	1.724(14)
C4′−B7′	1.747(3)	1.67(4)	1.738(14)
B7−C3	1.589(3)	1.66(3)	1.60(2)
B7′−C3′	1.588(3)	1.64(4)	1.593(14)
C3−B6	1.603(3)	1.57(3)	1.600(14)
C3′−B6′	1.610(3)	1.63(3)	1.628(14)
B6−B5	1.863(3)	1.72(4)	1.85(2)
B6′−B5′	1.867(3)	1.72(4)	1.83(2)
B5−C2	1.604(3)	1.60(4)	1.613(13)
B5′−C2′	1.605(3)	1.65(3)	1.623(14)

$$\underset{\textbf{7}}{1\text{-}(\eta^5\text{-}C_5H_5)\text{-}2\text{-}Ph\text{-}closo\text{-}1,2,3,4\text{-}FeC_3B_7H_9} + Cr(CO)_6 \rightarrow \underset{\textbf{9}}{1\text{-}(\eta^5\text{-}C_5H_5)\text{-}2\text{-}[(\eta^6\text{-}C_6H_5)Cr(CO)_3]\text{-}closo\text{-}1,2,3,4\text{-}FeC_3B_7H_9} + 3CO \quad (8)$$

Consistent with the withdrawing nature of the $Cr(CO)_3$ group coordinated to the cage phenyl substituent, the ^{11}B NMR spectrum of **9** is nearly identical to that of **7**, but with the peak positions shifted slightly downfield relative to those in **7**. In the ^1H NMR spectrum, the arene protons of **9** resonate at higher field than those in **7** and fall into the normal range observed in other (η^6-arene)$Cr(CO)_3$ complexes.[21]

As shown in Figure 7, a crystallographic determination of **9** showed that there are two independent molecules in the unit cell, with the two molecules differing in their relative orientations of the $Cr(CO)_3$ group with respect to the phenyl ring. Unsubstituted (η^6-arene)$Cr(CO)_3$ complexes have been found to exhibit two different arene/carbonyl conformations, where the carbonyl groups are oriented in the eclipsed or staggered forms.[21a,22] In the case of monosubstituted arene complexes (η^6-RC_6H_5)$Cr(CO)_3$, the eclipsed conformation can occur in either the *syn* or *anti* orientations. The conformations of the (-η^6-C_6H_5)$Cr(CO)_3$ fragments found in the

(19) Top, S.; Jaouen, G. *J. Organomet. Chem.* **1979**, *182*, 381−392.
(20) Mahaffy, C. A. L.; Pauson, P. L. *Inorg. Synth.* **1979**, *19*, 154−158.
(21) (a) Solladie-Cavallo, A. *Polyhedron* **1985**, *6*, 901−927. (b) Price, J. T.; Sorensen, T. S. *Can. J. Chem.* **1968**, *46*, 515−522. (c) Emanuel, R. V.; Randall, E. W. *J. Chem. Soc. (A)* **1969**, 3002−3006.
(22) Muetterties, E. L.; Bleeke, J. R.; Wucherer, E. J.; Albright, T. A. *Chem. Rev.* **1982**, *82*, 499−525.

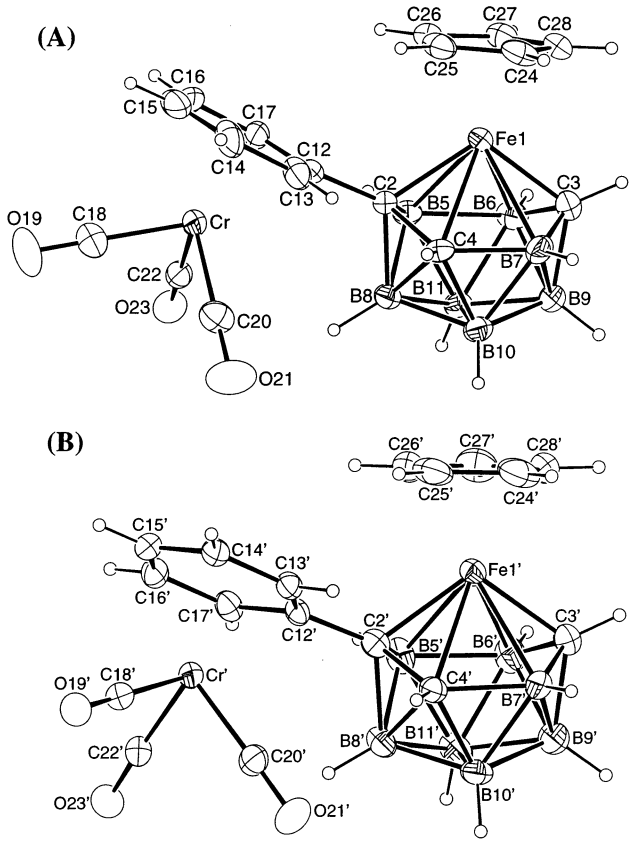

Figure 7. ORTEP drawings of the structures of the two independent molecules in the crystal structure of 1-(η^5-C_5H_5)-2-[(η^6-C_6H_5)$Cr(CO)_3$]-*closo*-1,2,3,4-$FeC_3B_7H_9$ (**9**).

two molecules of complex **9** are shown in Figure 8, where it can be seen that molecule **A** has the *anti* conformation, in which the Cr−CO bonds overlap with the phenyl-carbons at the *ortho* and *para* positions, while in molecule **B**, the unit has adopted a staggered conformation. The staggered structure adopted by molecule **B** is relatively uncommon for monosubstituted arenes, but has, in fact, been observed in another polyborane complex, *nido*-2,3-[$(CO)_3Cr(\eta^6$-$C_6H_5)CH_2]_2$-2,3-$C_2B_4H_6$.[23]

The intracage distances in **9** (Table 3) are quite similar to those found in **7**. Likewise, the bond lengths and angles observed in the (η^6-C_6H_5)$Cr(CO)_3$ fragments (Figure 8 caption), as well as the observed C≡O stretching frequencies (1965, 1894, 1872 cm^{-1}), are consistent with the values found in other (η^6-RC_6H_5)$Cr(CO)_3$ complexes.[21a,22]

Reversible Cage-Slippage Reactions. As shown in eqs 9 and 10, addition of excess *tert*-butyl isocyanide to glyme solutions of either 1-(η^5-C_5Me_5)-2-Me-*closo*-1,2,3,4-$RuC_3B_7H_9$ (**3**) (reddish-orange) or 1-(η^5-C_5H_5)-2-Ph-*closo*-1,2,3,4-$FeC_3B_7H_9$ (**7**) (blue) resulted in an immediate color change characteristic of the formation of the 8-(η^5-C_5Me_5)-8-($CNBu^t$)-9-Me-*nido*-8,7,9,10-$RuC_3B_7H_9$ (**10**) (yellow) and 8-(η^5-C_5H_5)-8-($CNBu^t$)-9-Ph-*nido*-8,7,9,10-$FeC_3B_7H_9$ (**11**) (brownish-red) products, respectively. Crystallization from the reaction solutions gave 97% and 62% isolated yields, respectively, of pure materials. Elemental analyses are consistent with the indicated

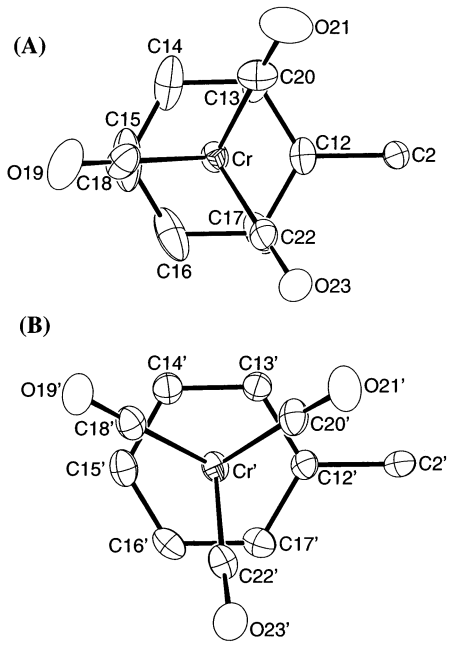

Figure 8. Expanded views of the *anti*-eclipsed and staggered conformations of the (-η^6-C_6H_5)$Cr(CO)_3$ fragments of the two independent molecules in the crystal structure of 1-(η^5-C_5H_5)-2-[(η^6-C_6H_5)$Cr(CO)_3$]-*closo*-1,2,3,4-$FeC_3B_7H_9$ (**9**). Selected distances (Å) and angles (deg) for (-η^6-C_6H_5)Cr-$(CO)_3$ fragments, structure **A** (*anti*-eclipsed): Cr−C18 1.830(6); Cr−C20 1.838(6); Cr−C22 1.830(6); C18−O19 1.162(6); C20−O21 1.158(7); C22−O23 1.166(6); C12−C13 1.415(7); C13−C14 1.415(7); C14−C15 1.397(11); C15−C16 1.389(11); C16−C17 1.415(8); C17−C12 1.412(7); Cr−ring centroid 1.7074(7); C18−Cr−C22 88.5(2); C18−Cr−C20 88.3(3); C20−Cr−C22 88.3(2); structure **B** (staggered): Cr′−C18′ 1.840(5); Cr′−C20′ 1.827(5); Cr′−C22′ 1.834(5); C18′−O19′ 1.167(6); C20′−O21′ 1.166(6); C22′−O23′ 1.166-(6); C12′−C13′ 1.436(6); C13′−C14′ 1.406(6); C14′−C15′ 1.412(7); C15′−C16′ 1.386(7); C16′−C17′ 1.415(7); C17′−C12′ 1.405(6); Cr′−ring centroid 1.7169(7); C18′−Cr′−C22′ 90.8(2); C18′−Cr′−C20′ 88.4(2); C20′−Cr′−C22′ 86.6(2).

compositions resulting from the association of 1 equiv of the *tert*-butyl isocyanide.

$$\underset{\textbf{3}}{\text{1-}(\eta^5\text{-}C_5Me_5)\text{-2-Me-}closo\text{-1,2,3,4-}RuC_3B_7H_9} + CNBu^t \rightleftharpoons \underset{\textbf{10}}{\text{8-}(\eta^5\text{-}C_5Me_5)\text{-8-}(CNBu^t)\text{-9-Me-}nido\text{-8,7,9,10-}RuC_3B_7H_9} \quad (9)$$

$$\underset{\textbf{7}}{\text{1-}(\eta^5\text{-}C_5H_5)\text{-2-Ph-}closo\text{-1,2,3,4-}FeC_3B_7H_9} + CNBu^t \rightleftharpoons \underset{\textbf{11}}{\text{8-}(\eta^5\text{-}C_5H_5)\text{-8-}(CNBu^t)\text{-9-Ph-}nido\text{-8,7,9,10-}FeC_3B_7H_9} \quad (10)$$

These reactions are reversible. Heating a toluene solution of **10** at reflux under flowing N_2 for 20 min resulted in the quantitative formation of **3**, while simply dissolving pure **11** in glyme resulted in the formation of an equilibrium mixture of **7** and **11**. Heating the solution to reflux under flowing N_2 resulted in complete conversion to **7**.

(23) Spencer, J. T.; Pourian, M. R.; Butcher, R. Y.; Sinn, E.; Grimes, R. N. *Organometallics* **1987**, *6*, 335−343.

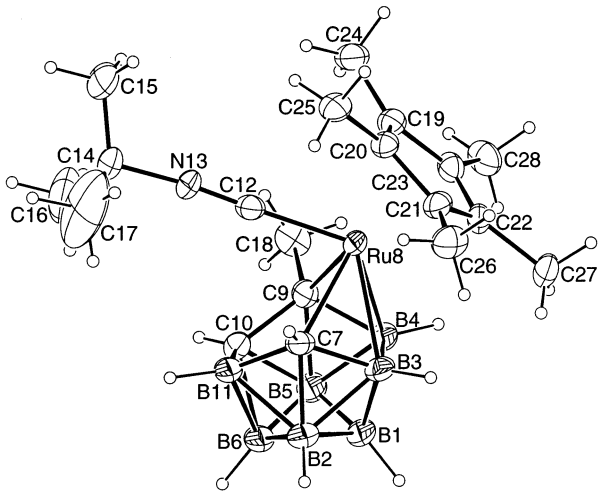

Figure 9. ORTEP drawing of the structure of 8-(η^5-C_5Me_5)-8-(CNBu^t)-9-Me-*nido*-8,7,9,10-$RuC_3B_7H_9$ (**10**).

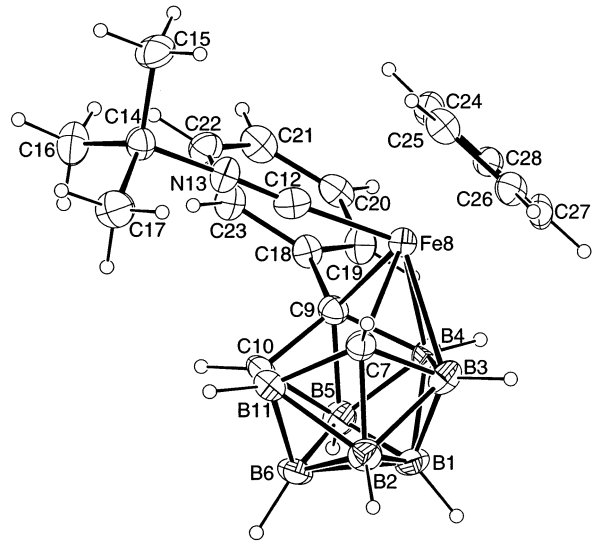

Figure 10. ORTEP drawing of the structure of 8-(η^5-C_5H_5)-8-(CNBu^t)-9-Ph-*nido*-8,7,9,10-$FeC_3B_7H_9$ (**11**).

The metals in **3**, **7**, and **8**, as in ruthenocene and ferrocene, have formal 18-electron counts. Thus, unless there is a change in the donor properties of either the cyclopentadienyl or tricarbadecaboranyl ligands, the metal coordination of a two-electron isocyanide ligand would result in the formation of a 20-electron complex. As shown in the ORTEP drawings in Figures 9 and 10, crystallographic studies of **10** and **11** demonstrated that upon isocyanide addition, the cyclopentadienyl rings remain symmetrically bonded to the metals with only a slight increase in the metal to ring-centroid distances in **10** (1.871(3) Å) and **11** (1.736(1) Å) relative to their values in **3** (1.829(2) Å) and **7** (1.695(3) Å), respectively (Table 5). However, the coordination mode of the tricarbadecaboranyl ligand in **10** and **11** has changed from η^6 to η^4. Thus, in **10** and **11**, the ruthenium and iron atoms are no longer centered over the six-membered face, but instead, the metals have slipped to one side of the cage. The metals are now centered above the C7−B3−B4−C9 face with the bond lengths between the metal and the four facial atoms being similar. Nonbonding distances (>3.0 Å) are found between the metals and the C10 and B11 cage atoms. In **7** and **8**, the M−C2−B8−B9−C3 atoms were coplanar, but in **10** and **11** the metals lie significantly out of the plane of the other four atoms, so that the dihedral angles between the C7−M−C9 and C7−B2−B5−C9 planes in **10** and **11** are 36.8(1)° and 36.3(3)°, respectively.

Table 5. Intramolecular Distances (Å) in Compounds 10 and 11 (M = Ru for 10 and Fe for 11)

bond	**10**	**11**
M−C9	2.204(6)	2.102(8)
M−C7	2.218(5)	2.114(8)
M−B4	2.246(5)	2.175(9)
M−B3	2.273(6)	2.191(9)
M−C10	3.117(6)	3.020(8)
M−B11	3.152(7)	3.051(10)
M−Cp/Cp*	1.871(3)	1.736(1)
C9−B4	1.632(8)	1.575(12)
B4−B3	1.875(10)	1.861(13)
B3−C7	1.605(9)	1.585(12)
C7−B11	1.588(9)	1.606(12)
B11−C10	1.639(10)	1.656(12)
C10−C9	1.541(8)	1.537(11)

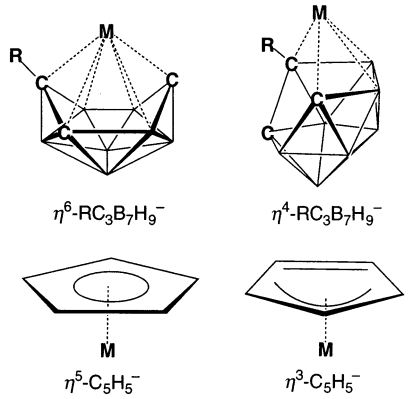

Figure 11. Comparison of structures and bonding modes of the tricarbadecaborane and cyclopentadienide monoanions.

As we have previously discussed,[3e,24] the change from the η^6- to η^4-coordination mode corresponds to a conversion of the tricarbadecaboranyl ligand from a six- to a four-electron donor. As illustrated in Figure 11, an η^4-tricarbadecaboranyl ligand could therefore be considered the electronic analogue of a metal-coordinated η^3-$C_3H_5^{1-}$ allyl or a "slipped" η^3-$C_5H_5^{1-}$ ligand. Thus, the net result of the addition of the two-electron isocyanide ligand to complexes **3** and **7** is to convert the tricarbadecaboranyl ligands to their η^4-coordination modes, reducing their electron donation to the metals to only four electrons and thereby preserving the metal's favorable 18-electron count.[25] From a skeletal-electron counting point of view,[17] this process simply corresponds to a cage-opening of the metallatricarbadecaboranyl fragment brought about by the addition of two electrons to the

(24) Weinmann, W.; Pritzkow, H.; Siebert, W.; Sneddon, L. G. *Chem. Ber./Recl.* **1997**, *130*, 329−333.

(25) Siebert has also shown that the diborolyl rings in the formal 16-electron complexes (η^5-C_5Me_5)Ru($R_3'C_3B_2R_2$) and (η^5-C_5H_5)Fe($R_3'C_3B_2R_2$) reversibly change their degree of folding upon the association/dissociation reactions of the complexes with *tert*-butyl isocyanide to form the 18-electron (η^5-C_5Me_5)Ru(CNBu^t)($R_3'C_3B_2R_2$) and (η^5-C_5H_5)Fe(CNBu^t)($R_3'C_3B_2R_2$) complexes. See: (a) Hettrich, R.; Kaschke, M.; Wadepohl, H.; Weinmann, W.; Stephan, M.; Pritzkow, H.; Siebert, W.; Hyla-Kryspin, I.; Gleiter, R. *Chem. Eur. J.* **1996**, *2*, 487−494. (b) Müller, T.; Kaschke, M.; Strauch, M.; Ginsberg, A.; Pritzkow, H.; Siebert, W. *Eur. J. Inorg. Chem.* **1999**, 1685−1692.

Table 6. Reversible Redox Potentials (V vs $Cp_2Fe^{0/+}$) of Relevant Metallatricarbadecaboranyl and Cyclopentadienyl Complexes in Nonaqueous Solutions Containing 0.1 M $[NBu_4][B(C_6F_5)_4]$

compound	solvent	$E_{1/2}(0/1+)$	$E_{1/2}(0/1-)$	$E_{1/2}(1-/2-)$	source
$CpFe(MeC_3B_7H_9)$, **12**	CH_2Cl_2[a]	0.39			ref 3g
$CpFe(MeC_3B_7H_9)$, **12**	THF		-1.74		ref 3g
$CpFe(PhC_3B_7H_9)$, **7**	CH_2Cl_2	0.43			this work
$CpFe(PhC_3B_7H_9)$, **7**	THF		−1.64	−2.79	this work
$Cp^*Ru(MeC_3B_7H_9)$, **3**	CH_2Cl_2	0.52			this work
$Cp^*Ru(MeC_3B_7H_9)$, **3**	THF		−2.32	−2.7 (irrev)[b]	this work
$Cp^*Ru(PhC_3B_7H_9)$, **8**	CH_2Cl_2	0.57			this work
$Cp^*Ru(PhC_3B_7H_9)$, **8**	THF		−2.18	−2.56	this work
$Ru(MeC_3B_7H_9)_2$, **4**	CH_2Cl_2	1.28	−1.33	−1.5	this work
$Os(MeC_3B_7H_9)_2$, **6**	THF	1.2_5 (irrev)[b]	−1.37	−1.52	this work
Cp_2Fe	THF	0	−3.4		ref 32[c]
Cp_2Ru	CH_2Cl_2	0.41			this work, ref 33[e]
Cp_2Ru	THF[a]		−3.9[d]		ref 34
Cp_2Os	CH_2Cl_2[e]	0.36			ref 33[c]
Cp_2Os	THF[a]		−3.9[d]		ref 34

[a] Supporting electrolyte was 0.1 M $[NBu_4][PF_6]$. [b] For chemically irreversible systems, $E_{1/2}$ is estimated from E_p at CV scan rate of 0.1 V/s. [c] Reduction of ferrocene at $T = 228$ K. [d] Value estimated from reduced temperature data in ref 32. [e] In experiments involving $[NBu_4][B(C_6H_3(CF_3)_2)_4]$ as supporting electrolyte, ref 33 reports $Cp_2Ru^{0/+}$ as 0.56 V and $Cp_2Os^{0/+}$ as 0.36 V vs ferrocene.

closo-$M(R)C_3B_7H_9$ cage (24 skeletal electrons) frameworks of **3** and **7** to form the *nido*-$M(R)C_3B_7H_9$ cage (26 skeletal electrons) structures of **10** and **11**.

No reaction was observed between *tert*-butylisocyanide and the *commo*-complex **4** (eq 11). Lack of reaction probably results from the fact that, as can be seen in the structure in Figure 4, the two tricarbadecaborane ligands in **4** are oriented in such a fashion that they wrap around the ruthenium and protect it from attack by the *tert*-butylisocyanide.

commo-Ru-(2-Me-*closo*-1,2,3,4-$RuC_3B_7H_9)_2$ + **4**

$CNBu^t \rightarrow$ No Reaction (11)

Although not observed for ferrocene and ruthenocene, reversible ring-slippage from η^5 to η^3 has been proposed, as shown in the well-studied example[6d,e] in eq 12, to be a key step in the substitution reactions of numerous cyclopentadienyl complexes[6] and some dicarbaboranyl complexes.[26]

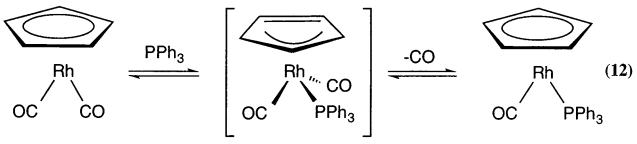

(12)

As discussed above for the tricarbadecaboranyl complexes, cyclopentadienyl η^5 to η^3 ring-slippage both provides an open coordination site for the incoming ligand and avoids the formation of an unfavorable 20-electron intermediate, thus providing a low-energy pathway for the substitution reaction. Similar cyclopentadienyl ring-slippages are thought to be critical steps in many other important stoichiometric and catalytic organometallic reactions.[6] The η^6 to η^4 cage-slippage reaction reported herein not only further illustrates the similarities of the cyclopentadienyl and tricarbadecaboranyl ligands but also demonstrates that tricarbadecaboranyl cage-slippage is preferred over η^5 to η^3 cyclopentadienyl ring-slippage in these complexes. The facile nature of the tricarbadecaboranyl rearrangement further suggests that metallatricarbadecaboranyl complexes may exhibit even greater reactivities than their cyclopentadienyl counterparts for many transformations requiring the generation of a coordinatively unsaturated metal center.

Electrochemical Studies. When compared with measured or estimated redox potentials of metallocene analogues, the redox reactions of compounds **3**, **4**, **6**, **7**, and **8** clearly show a tendency toward the thermodynamic stabilization of metals in lower oxidation states. Although this property has been noted previously,[3g] the present data allow quantification of the tricarbadecaboranyl electronic effect relative to that of the Cp ligand. Before discussing that however, we first summarize aspects of the chemical and electrochemical reversibilities of the redox reactions.

All five of the electrochemically investigated compounds give rise to three diffusion-controlled redox processes comprised of one oxidation and two reductions (Table 6). Each process has one-electron stoichiometry, as determined indirectly by comparison of their CV peak heights and ΔE_p values, and directly by coulometry (*vide infra*). These electron-transfer reactions generally approach Nernstian behavior,[27] implying relatively rapid heterogeneous electron-transfer reactions and allowing us to write eq 13 as a description of **4** and its analogues. Exceptions to completely reversible behavior will be discussed.

$$\mathbf{4}^+ \overset{-e^-}{\rightleftharpoons} \mathbf{4} \overset{+e^-}{\rightleftharpoons} \mathbf{4}^- \overset{+e^-}{\rightleftharpoons} \mathbf{4}^{2-} \qquad (13)$$

Bulk electrolyses carried out on the oxidation of **3** at room temperature and on the first reduction of **4** at 233 K confirmed the one-electron stoichiometries and showed that the products ($\mathbf{3}^+$ and $\mathbf{4}^-$, respectively) are reasonably persistent under these conditions. Regenerative electrolyses (e.g., "back"-oxidation of electrochemically generated $\mathbf{4}^-$) gave back the starting materials in 90% yield for **4** and 65% yield for **3**.

Variations in reversibility were primarily found in the cathodic reactions of these compounds. As demonstrated in Figure 12A, the CV response for the mixed-sandwich compound **8** reveals that the dianion $\mathbf{8}^{2-}$ undergoes a

(26) See for example: Shen, J. K.; Zhang, S.; Basolo, F.; Johnson, S. E.; Hawthorne, M. F. *Inorg. Chim. Acta* **1995**, *235*, 89−97.

(27) Except where noted, values of $|E_{pa} - E_{pc}|$ were very similar to those observed for the $Cp_2Fe^{+/0}$ couple under similar conditions.

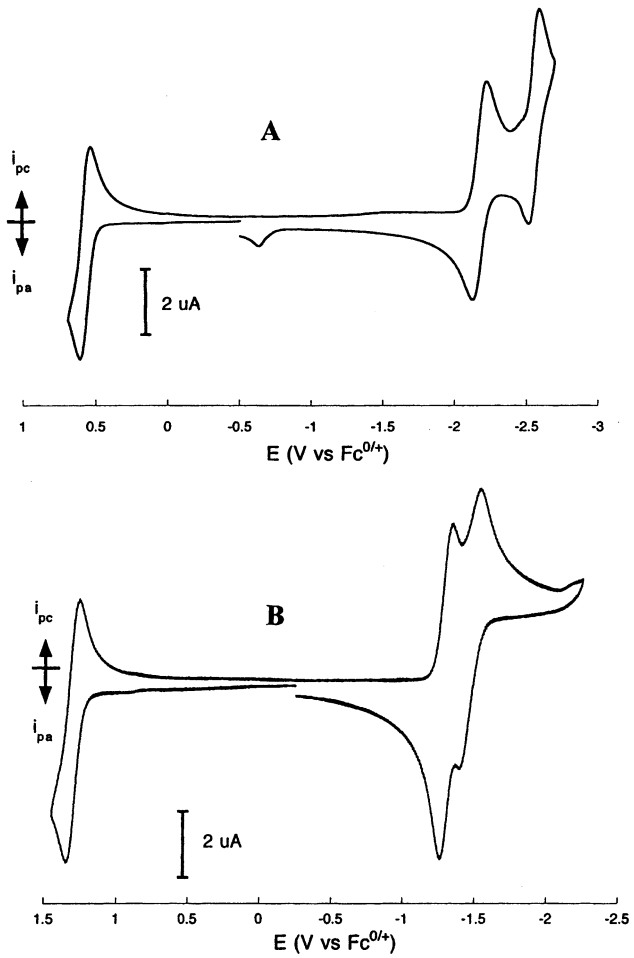

Figure 12. (A) Cyclic voltammogram of 2 mM 1-(η^5-C_5Me_5)-2-Ph-*closo*-1,2,3,4-$RuC_3B_7H_9$ (**8**) in CH_2Cl_2/0.1 M $[NBu_4][B(C_6F_5)_4]$ at d = 2 mm glassy carbon electrode. Room temperature, 0.2 V/s. (B) Cyclic voltammogram of 1 mM *commo-Ru*-(2-Me-*closo*-1,2,3,4-$RuC_3B_7H_9)_2$ (**4**) in CH_2Cl_2/0.1M $[NBu_4][B(C_6F_5)_4]$ at d = 2 mm glassy carbon electrode. Room temperature, 0.2 V/s.

follow-up reaction to produce a product with an oxidation wave at ca. −0.65 V. A similar result was found for the second reduction of **3**. The only indication of electrochemical quasi-reversibility (i.e., a slow heterogeneous charge transfer) was observed in the second reduction of the Ru bis-caged system $\mathbf{4}^{1-/2-}$ (see second cathodic wave in Figure 12B). The $\mathbf{4}^{1-/2-}$ process exhibits its effects from changes in solvent, temperature, and scan rate, details of which are under investigation. Perusal of the $E_{1/2}$ values in Table 6 confirms that each electron-transfer process of a mono- or bis-cage compound is shifted positive compared to the equivalent process of its metallocene analogue.[28] It is readily apparent, however, that the positive shifts for the first *reduction* of the neutral compounds (i.e., the 0/1− couple) are much greater than those seen for the *oxidation* of the same compound (i.e., the 0/1+ couple). This shows that the potential shifts of the *cathodic reactions* cannot be ascribed to an electronic effect analogous, for example, to the inductive effect observed in the replacement of a C_5H_5 ligand by a C_5Me_5 ligand. A measure of the comparative inductive effect upon

(28) See Experimental Section for summary of metallocene potentials.

Table 7. $E_{1/2}$(0/1+) and $E_{1/2}$(0/1−) Shifts (V) for Tricarbadecaboranyl Complexes Compared to Identical Couples of Metallocene Analogues

compound	$\Delta E_{1/2}$ (ox)[a]	shift per lig[b]	$\Delta E_{1/2}$ (red)[c]	excess shift[d]
12	0.39	0.39	1.66	1.22
7	0.43	0.43	1.76	1.32
3	0.41	0.41	1.88	1.44
8	0.46	0.46	2.02	1.58
4	0.87	0.43_5	2.57	1.69
6	∼1[e]	∼0.5[e]	2.53	1.65

[a] $E_{1/2}$(0/1+) for compound minus $E_{1/2}$(0/1+) for analogous Cp_2M. [b] lig = $RC_3B_7H_9$. [c] $E_{1/2}$(0/1−) for compound minus $E_{1/2}$(0/1−) for analogous Cp_2M. [d] $\Delta E_{1/2}$ (red) minus [m × (0.044 V)], where m is number of $RC_3B_7H_9$ ligands. [e] Estimated from peak potential of irreversible oxidation of **6** in THF.

replacement of a Cp by $RC_3B_7H_9$ is obtained by comparison of the $\Delta E_{1/2}$(0/1+) values in Table 6, where $\Delta E_{1/2}(0/1+) = [E_{1/2}(0/1+)$ of $(RC_3B_7H_9)_mCp_{2-m}M) - E_{1/2}(0/1+)$ of $(Cp_2M)]$, m = 1, 2. In each case, the neutral compound is an 18-electron system which is not expected to undergo significant structural changes upon one-electron oxidation. As shown in Table 7, the $\Delta E_{1/2}$(0/1+) value for six $RC_3B_7H_9$-containing compounds is 0.44 ± 0.04 V for each substitution of a Cp group by an $RC_3B_7H_9$ group.[29] We therefore use the value of 0.44 V as the comparative inductive effect of the $RC_3B_7H_9$ group in the iron-group complexes.

For comparison, a comparative electronic effect of ca. −0.25 V was obtained for the dicarbollide ligand, $[C_2B_9H_{11}]^{2-}$, when compared to Cp^-,[18a,30] the negative sign being consistent in that case with the stabilization of *higher* oxidation states by the more negatively charged $[C_2B_9H_{11}]^{2-}$ ligand.[18a] Significantly, the −0.25 V dicarbollide comparative inductive effect successfully accounted for trends in both the oxidations *and* reductions of neutral compounds,[30] in contrast to the present findings for tricarbadecaboranyl complexes. The additional stabilization for the first reductions of the tricarbadecaboranyl complexes is quantified by subtracting the amount (0.44 × m)volt from the measured shifts in $E_{1/2}$(0/1−), where m is the number of $RC_3B_7H_9$ ligands in the compound (see Table 7). For example, compared to the reduction of ruthenocene ($Cp_2Ru^{0/1-}$), the $E_{1/2}$ of $[(MeC_3B_7H_9)_2Ru]^{0/1-}$, $\mathbf{4}^{0/1-}$, is more positive by 2.57 V. About 0.88 V of this value is accounted for by the replacement of two Cp rings in Cp_2Ru by $RC_3B_7H_9$ ligands in **4**. This leaves an additional stabilization (excess shift) of about 1.69 V, which must arise from factors other than the comparative inductive effect. Using this approach, one finds an additional stabilization of 1.2−1.3 V for the two Fe compounds and 1.4−1.7 V for the Ru and Os compounds (Table 7). Furthermore, these data suggest that the great bulk of the additional stabilization is found in substitution of the *first* Cp ligand by a $RC_3B_7H_9$ group.

Among the chemical factors that might be considered as contributing to the additional stabilization are (i) medium effects such as solvation and ion-pairing; (ii) changes in metal configurations or spin states, and (iii) structural changes that are coupled to the electron-transfer reactions. Given the results discussed above

(29) This value was adjusted by 0.3 V for compounds **3** and **8**, which contain Cp* groups.

(30) Geiger, W. E. In *Metal Interactions with Boron Clusters*; Grimes, R. N., Ed.; Plenum Press: New York, 1982; p 239.

demonstrating that the $RC_3B_7H_9$ ligand can change from a six-electron, η^6- to a four-electron, η^4-coordination mode upon the addition of a two-electron donor (see compounds **10** and **11**), a redox-induced structural change (i.e., possibility iii, specifically a slippage to lower than η^6-coordination) must be considered to be likely in the reduced tricarbadecaboranyl-containing complexes.

Much of the literature in which electrochemistry has been used to probe η^6/η^4 and η^5/η^3 bonding changes has been recently summarized.[31] These papers emphasize that heterogeneous electron-transfer rates are likely to be less intricate probes of structural reorganizations than are $E_{1/2}$ effects. More detailed mechanistic studies, including measurement of k_s values, are therefore planned for these and related η^n-$RC_3B_7H_9$ compounds. It should also be noted that the overall ligand-induced stabilization of reduced forms of metal-tricarbadecaboranyl complexes allows detection of formal metal oxidation states which seem to have no precedent in their metallocene analogues, namely, formal M^0 complexes, M = Fe, Ru, Os, in the dianions of compounds **3**, **4**, **6**, **7**, and **8**.

Acknowledgment. The National Science Foundation supported the research carried out at the Universities of Pennsylvania (CHE 98-14252) and Vermont (CHE 97-05763).

Supporting Information Available: X-ray crystallographic data for structure determinations of **4**, **5**, **6**, **7**, **8**, **9**, **10**, and **11** (CIF). This material is available free of charge via the Internet at http://pubs.acs.org.

OM020757U

(31) (a) Stoll, M. E.; Baelanzoni, P.; Calhorda, M. J.; Drew, M. G. B.; Felix, V.; Geiger, W. E.; Gamelas, C. A.; Gonzalves, I. S.; Romão, C. C.; Veiros, L. F. *J. Am. Chem. Soc.* **2001**, *123*, 10595−10606. (b) Geiger, W. E. *Acc. Chem. Res.* **1995**, *28*, 351−357.

(32) Ito, N.; Saji, T.; Aoyagui, S. *J. Organomet. Chem.* **1983**, *247*, 301−305.

(33) Hill, M. G.; Lamanna, W. G.; Mann, K. R. *Inorg. Chem.* **1991**, *30*, 4687−4690.

(34) Strelets, V. V. *Coord. Chem. Rev.* **1992**, *114*, 1−60.